Asian Journal of Chemistry; Vol. 35, No. 10 (2023), 2487-2492

ASIAN JOURNAL OF CHEMISTRY

https://doi.org/10.14233/ajchem.2023.28055

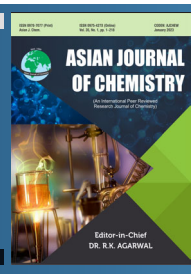

Optimization of Reaction Parameters during the Synthesis of Hexagonal Hexadecylamine Capped ZnS Nanoparticles

ABERA MADISHA JAWORE[1], THOKOZANI XABA[1,*], ZONDI NATE[1], TSHEPO NTSOANE[2] and MAKWENA JUSTICE MOLOTO[3]

[1]Department of Biotechnology and Chemistry, Vaal University of Technology, P/Bag X021, Vanderbijlpark, South Africa
[2]Applied Radiation, Research and Innovation, South African Nuclear Energy Corporation South Africa, Pretoria 0001, South Africa
[3]Institute for Nanotechnology and Water Sustainability, College of Science, Engineering and Technology, University of South Africa, Florida Science Campus, 1710, South Africa

*Corresponding author: E-mail: thokozanix@vut.ac.za

Received: 30 May 2023; *Accepted*: 17 August 2023; *Published online*: 28 September 2023; AJC-21401

Zinc sulphide nanoparticles capped with hexadecylamine (ZnS-HDA) have been synthesized through thermal decomposition of (*Z*)-2-(pyrrolidin-2-ylidene)thiourea zinc(II) complex. The effects of temperature, time and concentration of the precursor on the properties of ZnS-HDA capped nanoparticles were investigated. The values of the optical band edges were increasing when the temperature, reaction time and the amount of the precursor were elevated. X-ray diffraction patterns of all the synthesized nanoparticles mainly exhibited hexagonal phase structures. The morphologies of the particles were increasing with the increase in temperature, time and precursor concentration.

Keywords: Synthesis, Zinc sulfide nanoparticles, Substituted thiourea, Hexagonal phase.

INTRODUCTION

Extensive research has been conducted on semiconductor nanoparticles (NPs), particularly those belonging to group II-VI, owing to their distinctive features that hold significant appeal in several sectors such as electronics, sensing, photocatalysis, optics, *etc*. [1]. Amongst group II-VI semiconductor materials, ZnS has gained much attention due to its multiplicity of attractive luminescent properties [2]. Gallium nitride (GaN) is a significant component within the wide-gap semiconductor category [3]. Due of its multifaceted applications, this particular topic has garnered significant attention from researchers particularly in the field of optical sensors and coating, infrared window, reflector, dielectric filter, solar cells, *etc*. [4-6].

Zinc sulfide (ZnS) exists into two allotropic forms, a cubic sphalerite structure and a hexagonal wurtzite structure [7,8]. Several methods have been used to synthesize ZnS nanoparticles to produce nanostructured materials such as nanorods, nanosheets, nanotubes, nanobelts, nanocluster, nanorods, nanoflower, hollow sphere, nanowires, *etc*. [9]. These methods include sol-gel [10], hydrothermal [11], solvothermal [12], chemical precipitation [4], co-precipitation [13], chemical vapour deposition [14], homogeneous precipitation [15], *etc*.

Hoa *et al*. [16] employed a hydrothermal technique at 220 ºC to synthesize ZnS nanoparticles using various molar ratios of zinc and sulfur. The resulting nanoparticles exhibited characteristics consistent with the cubic zinc blende phase of ZnS. Whereas Zhao *et al*. [3] reported a novel and facile low temperature synthesis of monodispersed hexagonal ZnS nanoparticles annealed at different temperatures that had an average size of less than 5 nm. Abdullah *et al*. [17] reported the synthesis of zinc sulphide nanoparticles through the thermal breakdown of a complex involving zinc *N*-ethyl cyclohexyl dithiocarbamate at different calcined temperatures and reaction times results in the high purity of hexagonal wurtzite ZnS.

This work is mainly focused on the synthesis and characterization of ZnS nanoparticles capped with hexadecylamine by thermal decomposition method using (*Z*)-2-(pyrrolidin-2-ylidene)thiourea zinc(II) complex as a precursor. The effect of temperature, time and concentration of the precursor were studied during the synthetic process. The optical and structural

properties of the synthesized hexadecylamine capped zinc sulfide nanoparticles were also investigated.

EXPERIMENTAL

The chemicals *viz*. pyrrolidone, thiourea, zinc(II) chloride dihydrate, oleylamine, hexadecylamine, ethanol, methanol, toluene and acetone were procured from Sigma-Aldrich and used without further purification.

Characterization: UV-1800 Shimadzu spectrophotometer and Gilden Fluorescence were used to measure the optical properties of the synthesized zinc sulfide nanoparticles. The XRD patterns of the nanoparticles were obtained on a Phillips X'Pert diffractometer using secondary monochromated Cu *K*α radiation (λ = 1.54060 Å) at 40 Kv/30 mA. The Tecnai F30 FEG TEM instrument was used to take the transmission electron microscopy (TEM) images at 300 kV.

Synthesis of (*Z*)-2-(pyrrolidin-2-ylidene)thiourea zinc(II) complex: (*Z*)-2-(Pyrrolidin-2-ylidene)thiourea ligand was synthesized according to the reported method [15]. In brief, thiourea ligand (2 mmol) in an ethanolic solution (20 mL) was mixed with an ethanolic solution of zinc(II) chloride (1 mmol) and then the reaction mixture was refluxed for 3 h at 50 ºC (**Scheme-I**). The solution was then allowed to cool at room temperature and the precipitate was filtered, washed with ethanol and then dried in an open air. The complex was obtained as white powder. Yield: 78.3%; m.p. 273 ºC; Elemental analysis calcd. (found) % for $C_{10}H_{18}N_6S_2Cl_2Zn$: C, 28.42 (27.62); H, 4.29 (4.05); N, 19.88 (18.97); S, 15.17 (14.39).

Synthesis of hexadecylamine capped zinc sulfide nanoparticles: Exactly 1 g of Zn(II) complex was dissolved with oleylamine (5 mL) in a small beaker. Hexadecylamine (HDA) (5 g) was transferred into a 100 mL three-necked flask and heated in nitrogen gas atmosphere to a reaction temperature of 120 ºC. The dissolved Zn(II) complex was then injected into hot hexadecylamine and the reaction was allowed to proceed for 1 h at the same temperature. The resulting solution was then cooled to 70 ºC and about 20 mL of methanol was added into the flask. The resultant precipitate was separated using centrifugation technique by further addition of methanol. The product was washed several times with methanol, dried in an open air and characterized. The same procedure was repeated 160 and 200 ºC instead of 120 °C to investigate the effect of temperature and 0.5 g of Zn(II) complex was used instead of 1.0 g to study the effect of concentration. To study the effect of time, above procedure was repeated for 2 h instead of 1 h using 1.0 g of Zn(II) complex at 160 ºC.

RESULTS AND DISCUSSION

FTIR and thermogravimetric analysis: Fig. 1a shows the FTIR of (*Z*)-2-(pyrrolidin-2-ylidene)thiourea as ligand and its Zn complex with the peaks between 3457-3044 cm^{-1}, which are assigned to O–H stretching as well as a peak at 2708 cm^{-1} corresponds to the C-H stretch. The appearance of peak at 1627 cm^{-1} may be attributed to the N–H bending and a peak at 466 cm^{-1} also appeared which is due to the metal sulfide (Zn-S).

The thermal properties of (*Z*)-2-(pyrrolidin-2-ylidene)-thiourea zinc(II) complex was studied by thermogravimetric analysis at the temperature range from 20 to 800 ºC under nitrogen atmosphere. Fig. 1b shows the four decomposition stages of the synthesized zinc complex. The first three decomposition at the temperature range between 179-328 ºC with a weight loss 53.4% might be attributed due to the OH group of ethanol that was used for washing the complex. The final decomposition occurred between 328-566 ºC with final residue 12.54% maybe attributed to the loss of Zn–N.

Effect of temperature

Optical properties of HDA capped ZnS nanoparticles: The optical absorption measurements of HDA capped ZnS nanoparticles synthesized at 120, 160 and 200 ºC and their corresponding energy band gaps are shown in Fig. 2a. The synthesized samples show strong absorptions band edges at 326 nm (3.8 eV), 328 nm (3.78 eV) and 329 nm (3.77 eV), respectively. All the absorption wavelengths were blue shifted compared to the bulk ZnS (340 nm), which can be attributed to the quantum confinement effect [18,19]. The emission spectra of the HDA capped ZnS nanoparticles are shown in Fig. 2b. The photoluminescence spectra with the excitation wavelength of 350 nm, projected two emission maxima at 409 nm and 434 nm for all the synthesized nanoparticles.

Structural properties: The XRD patterns of the synthesized HDA capped ZnS nanoparticles at different reaction temperatures are shown in Fig. 3a. All the ZnS-HDA capped nanoparticles synthesized at 120 ºC, 160 ºC and 200 ºC mainly

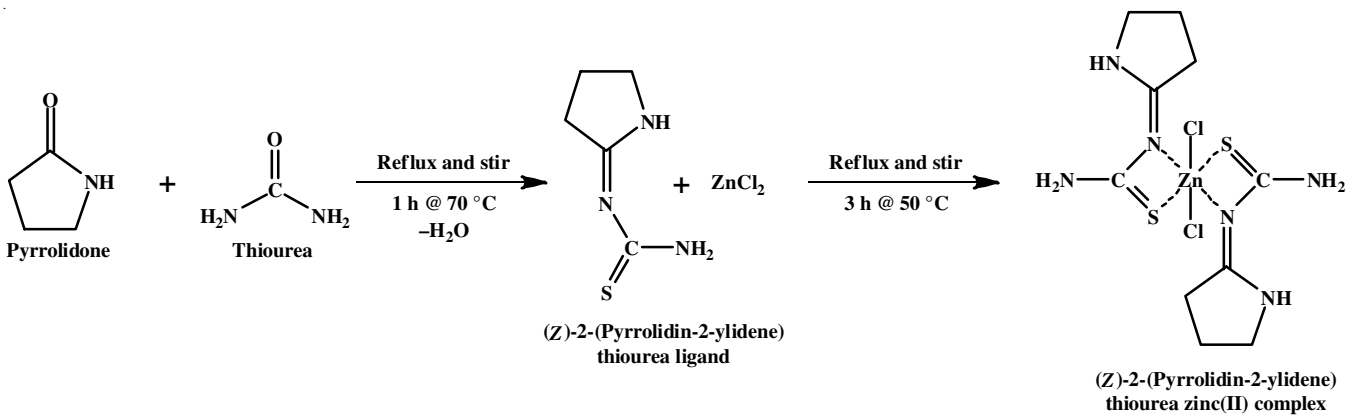

Scheme-I: Preparation of (*Z*)-2-(pyrrolidin-2-ylidene) thiourea ligand and (*Z*)-2-(pyrrolidin-2-ylidene) thiourea zinc(II) complex

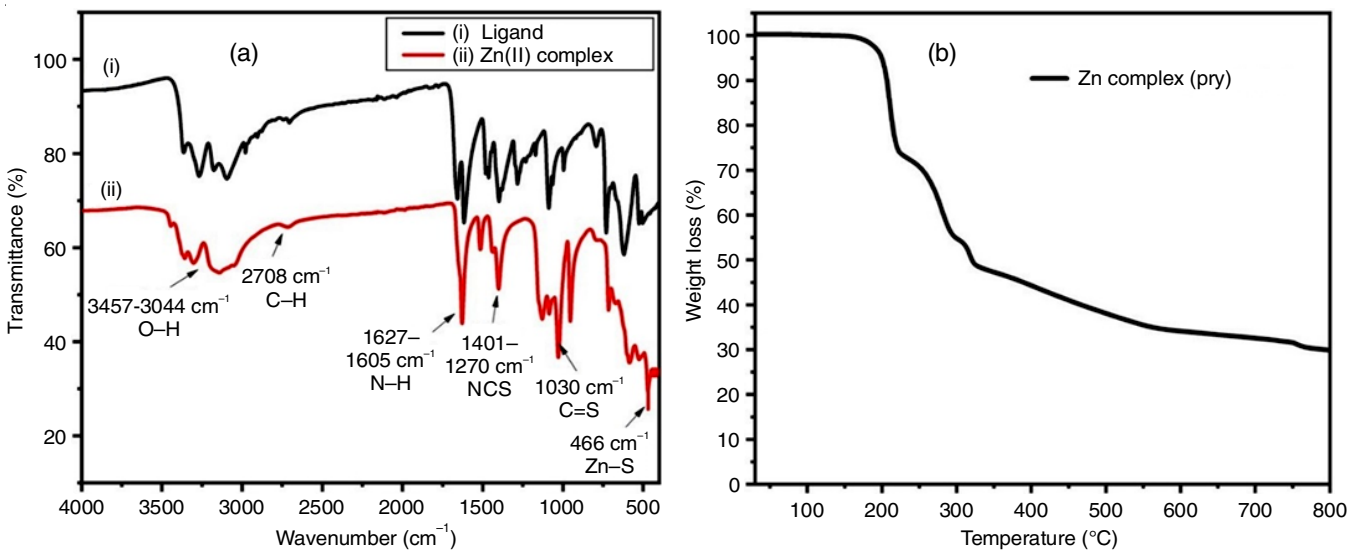

Fig. 1. FTIR spectra of (*Z*)-2-(pyrrolidin-2-ylidene) thiourea ligand & zinc(II) complex (a) and TGA curve for zinc(II) complex (b)

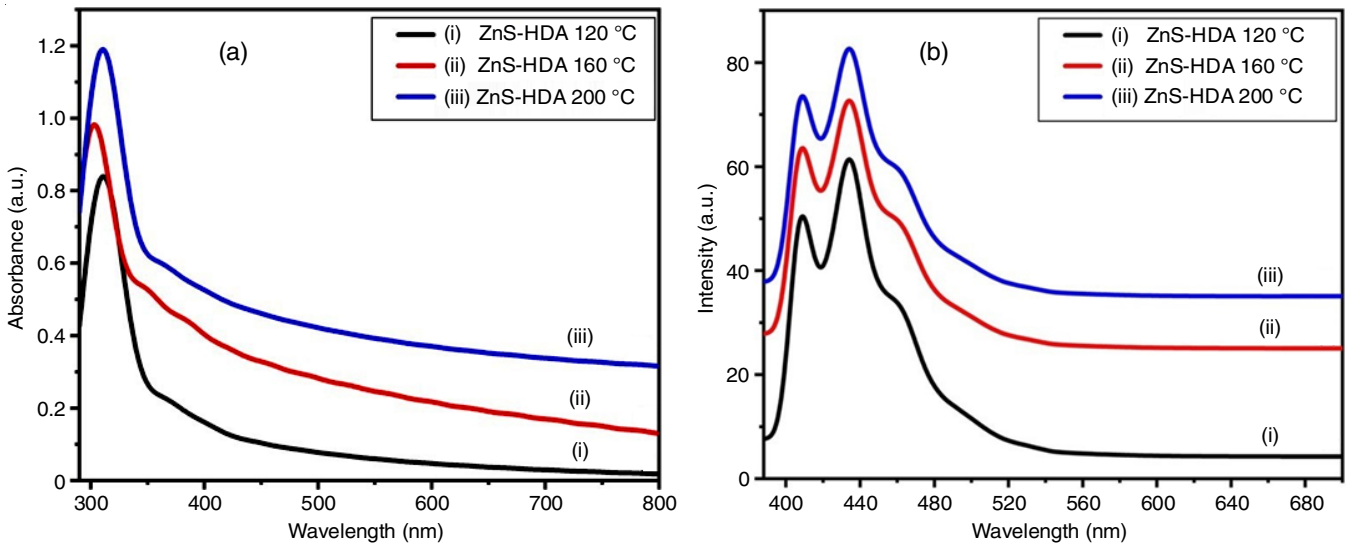

Fig. 2. UV-Vis (a) and emission (b) spectra of the HDA capped ZnS nanoparticles synthesized from (*Z*)-2-(pyrrolidin-2-ylidene) thiourea zinc(II) complex synthesized at 120 °C (i), 160 °C (ii) and 200 °C (iii)

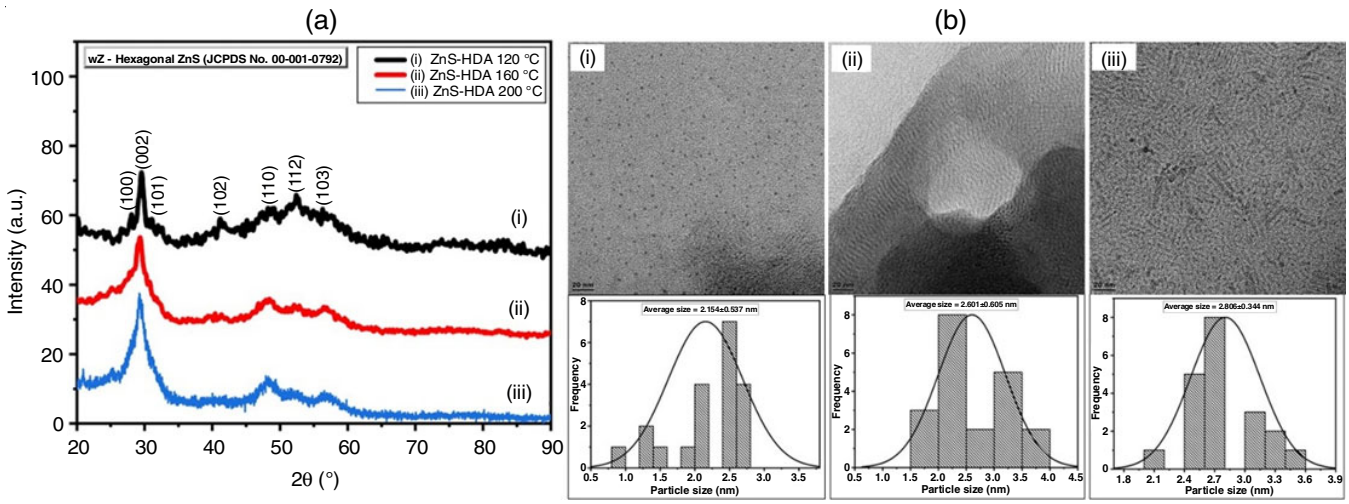

Fig. 3. XRD patterns (a) and TEM images (b) of the HDA capped ZnS nanoparticles synthesized from (*Z*)-2-(pyrrolidin-2-ylidene) thiourea zinc(II) complex at 120 ºC (i), 160 ºC (ii) and 200 ºC (iii)

exhibited peaks that correspond to (100), (002), (101), (102), (110), (112) and (103) planes that well-matched with the hexagonal phase, which correspond to the lattice constant according to literature (JCPDS card no. 00-001-0792) [20].

The broadening of the XRD patterns of the synthesized ZnS nanoparticles indicates the formation of small size particles. The average crystallite sizes were calculated using the Debye Scherrer's formula (eqn. 1) [21,22]:

$$d = \frac{0.9\lambda}{\beta\cos\theta}$$

where λ is wavelength (1.5418 Å) and β is the full width half maximum (FWHM) of corresponding peak. The calculated crystallite size of the synthesized ZnS nanoparticles were between 2.46-2.48 nm, which is also in good agreement with the TEM results.

The TEM images and their corresponding size distribution histograms of the HDA capped ZnS nanoparticles synthesized at different temperatures are shown in Fig. 3b. TEM images showed spherical shaped particles with the average particle sizes of 2.15, 2.60 and 2.81 nm, respectively. It was also observed that the particle sizes increased with the increase in temperature.

Effect of concentration of the precursor

Optical properties: Fig. 4a shows the absorption spectra of ZnS nanoparticles capped with HDA at different concentrations (*i.e.* 0.5 g and 1.0 g) of zinc(II) complex at 160 ºC. The absorption band edges of HDA capped ZnS nanoparticles was increasing slightly as the concentration of the precursor was increased and located at 327 nm (3.79 eV) and 328 nm (3.78 eV).

The emission spectra of HDA capped ZnS nanoparticles synthesized from the different concentrations of Zn(II) complex at the excitation wavelength of 350 nm at 160 ºC for 1 h are shown in Fig. 4b. The emission spectra projected two narrow emission peaks at 408 & 434 nm for the lower concentration and 409 & 434 nm for the higher concentration. The presence of narrow emission peaks is evidence of the distribution of small size particles [23].

Structural properties of HDA capped ZnS nanoparticles: The XRD spectrum for HDA capped ZnS nanoparticles synthesized at different concentrations of the precursor at 160 ºC for 1 h is represented in Fig. 5a. All the XRD patterns of the synthesized ZnS nanoparticles exhibited peaks that correspond to (100), (002), (101), (102), (110), (112) and (103) planes that well-matched with the pure hexagonal phase which correspond to JCPDS card no.: 00-001-0792. Minor impurity peaks were observed in the pattern of ZnS-HDA nanoparticles synthesized at higher concentration. This might be due to the unreacted moiety of the zinc(II) complex.

The shapes and the sizes of the synthesized HDA capped ZnS nanoparticles at different concentrations of the precursor were investigated with transmission electron microscopy (TEM). Fig. 5b showed the traces of the spherical particles with the average diameters of 2.607 and 2.617 nm. An increase in the diameter of the particle size as the concentration of the precursor is increased confirms the results that were obtained from the optical measurements.

Effect of reaction time

Optical properties: The absorption spectra of the synthesized HDA capped ZnS nanoparticles at different reaction times using of 1 h and 2 h at 160 ºC is shown in Fig. 6a. It was observed that the absorption band edges tend to increase when the reaction time was increased. The band edges appeared at 328 nm (3.78 eV) and 330 nm (3.76 eV) for 1 h and 2 h, respectively. An increase in the particle sizes with reaction time is due to the Ostwald ripening of the nuclei [24]. Fig. 6b revealed two emission peaks at 408 & 433 nm and 409 & 434 nm for the HDA capped ZnS nanoparticles synthesized at 1 and 2 h at the excitation wavelength of 350 nm. The narrow emission peaks are indication of small size particle distribution.

Structural properties: The XRD patterns of the synthesized HDA capped ZnS nanoparticles at different reaction times are shown in Fig. 7a. The nanoparticles synthesized for

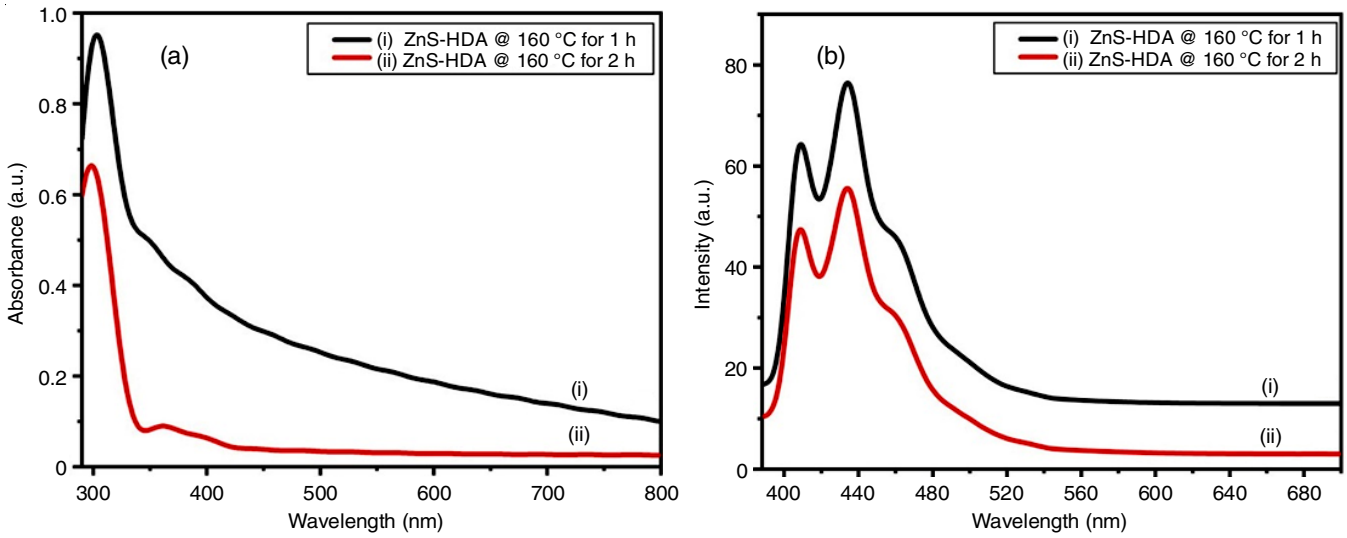

Fig. 4. UV-Vis (a) and photoluminescence (b) spectra of the HDA capped ZnS nanoparticles synthesized from the precursor concentrations of 0.5 g (i) and 1.0 g (ii)

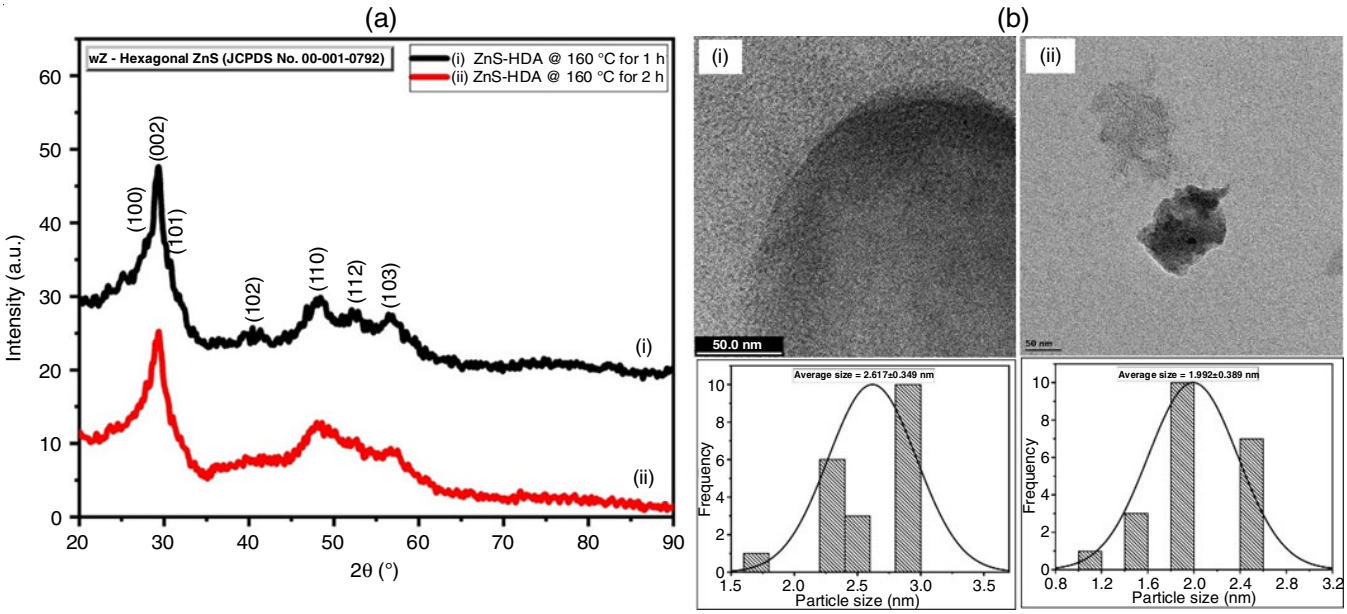

Fig. 5. X-ray diffraction patterns (a) and TEM images (b) of the HDA capped ZnS nanoparticles synthesized from the precursor concentrations of 0.5 g (i) and 1.0 g (ii)

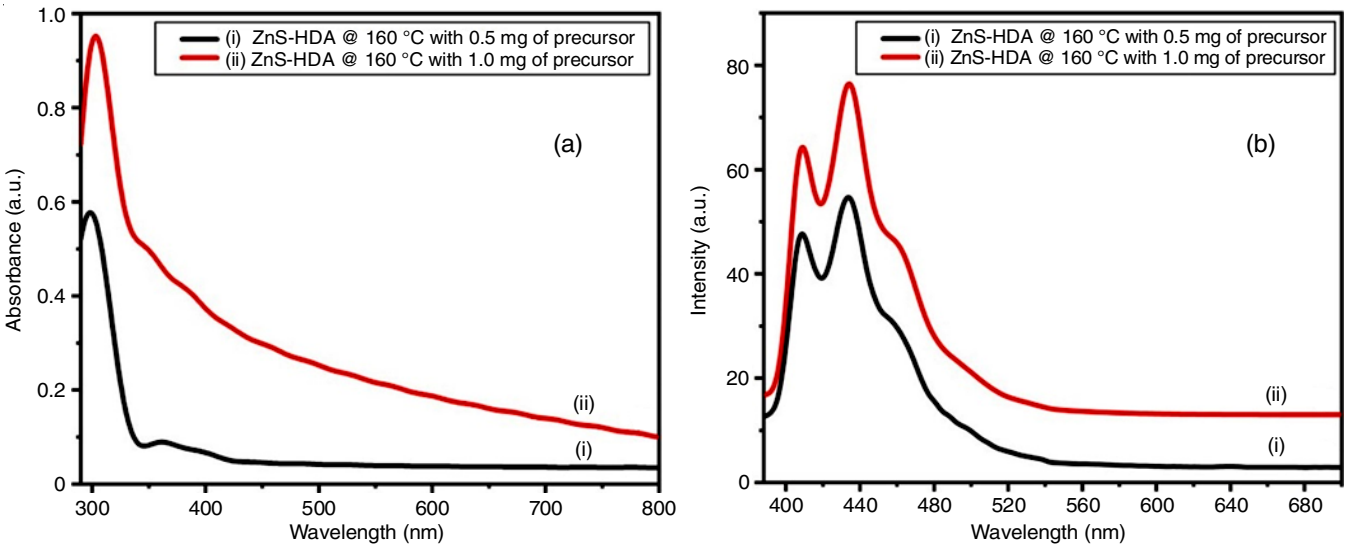

Fig. 6. UV-Vis (a) and photoluminescence (b) spectra of the HDA capped ZnS nanoparticles synthesized at 1 h (i) and 2 h (ii)

1 h and 2 h at 160 ºC exhibited peaks that correspond to (100), (002), (101), (102), (110), (112) and (103) planes that correspond with the pure hexagonal phase with JCPDS card no.: 00-001-0792. The pattern of the nanoparticles that were prepared after 1 h revealed strong peaks, but these peaks did not emerge in the pattern of the nanoparticles that were synthesized for a longer period of time. The transmission electron microscopy (TEM) images of the synthesized nanoparticles at different times is shown in Fig. 7b. All the synthesized HDA capped ZnS nanoparticles showed spherical particles. It was observed that when the reaction time was increased, the sizes of the particles were also increased with the average particle sizes of 2.62 and 2.64 nm.

Conclusion

The synthesis of (*Z*)-2-(pyrrolidin-2-ylidene)thiourea zinc(II) complex and ZnS nanoparticles capped with HDA have been accomplished through the thermolysis of zinc(II) complex at different temperatures, time and concentrations. The optical absorption spectra of the synthesized hexadecylamine (HDA) capped ZnS nanoparticles were blue-shifted from their bulk ZnS counterpart. X-ray diffraction analysis showed that the synthesized nanoparticles at higher temperature have a cubic zinc blende structure. Meanwhile, the transmission electron microscopy (TEM) images revealed spherical-shaped particles that increased in size when the reaction parameters were increased. This is an indication that the size of the crystallites can be adjusted by controlling the concentration, temperature and time.

ACKNOWLEDGEMENTS

The authors acknowledge the Vaal University of Technology and National Research Foundation (TTK13071722088: Thuthuka Grant Holder) for funding this project.

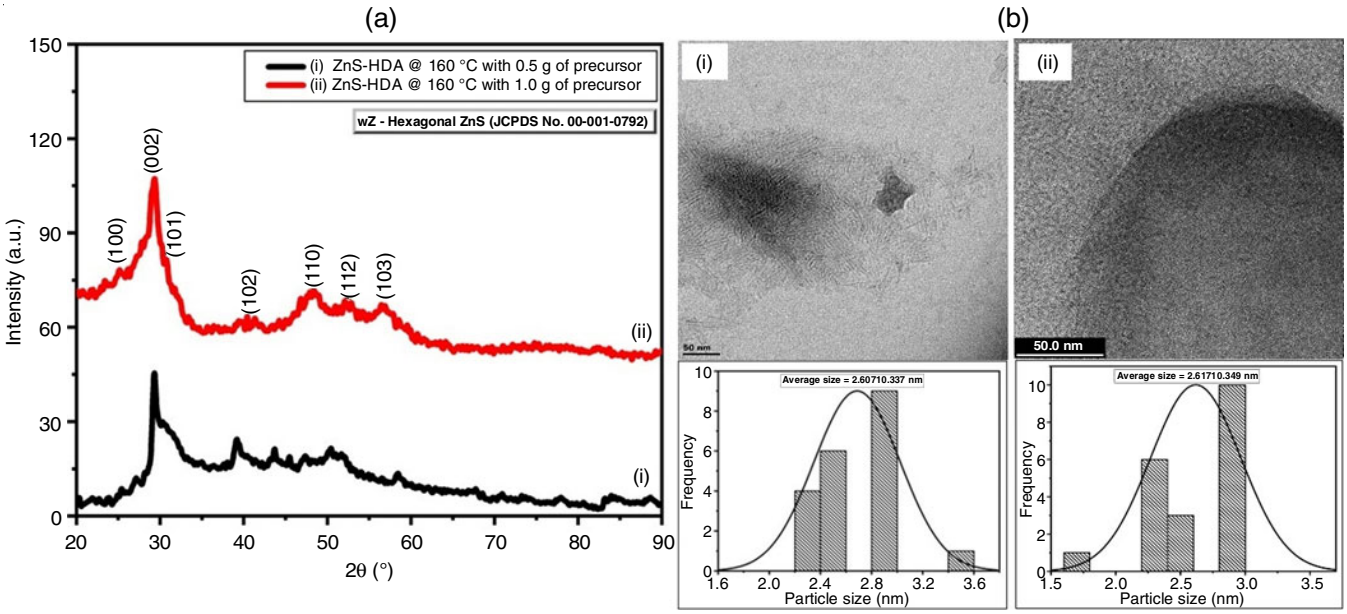

Fig. 7. X-ray diffraction patterns (a) and TEM images (b) of the HDA capped ZnS nanoparticles synthesized at 1 h (i) and 2 h (ii)

CONFLICT OF INTEREST

The authors declare that there is no conflict of interests regarding the publication of this article.

REFERENCES

1. N. Mintcheva, G. Gicheva, M. Panayotova and S.A. Kulinich, *Materials*, **13**, 171 (2020); https://doi.org/10.3390/ma13010171
2. C.S. Tiwary, P. Kumbhakar, A.K. Mitra and K. Chattopadhyay, *J. Lumin.*, **129**, 1366 (2009); https://doi.org/10.1016/j.jlumin.2009.07.004
3. Y. Zhao, Y. Zhang, H. Zhu, G.C. Hadjipanayis and J.Q. Xiao, *J. Am. Chem. Soc.*, **126**, 6874 (2004); https://doi.org/10.1021/ja048650g
4. Z.H. Hamed, K.E.A. Ahmed and H.A. Elsheikh, *Aswan Univ. J. Environ. Stud.*, **2**, 147 (2021); https://doi.org/10.21608/AUJES.2021.66918.1014
5. H.Y. Lu, S.Y. Chu and S.S. Tan, *J. Cryst. Growth*, **269**, 385 (2004); https://doi.org/10.1016/j.jcrysgro.2004.05.050
6. T.-F. Yi, Y. Li, Y.-M. Li, S. Luo and Y.-G. Liu, *Solid State Ion.*, **343**, 115074 (2019); https://doi.org/10.1016/j.ssi.2019.115074
7. H. Chen, D. Shi, J. Qi, J. Jia and B. Wang, *Phys. Lett. A*, **373**, 371 (2009); https://doi.org/10.1016/j.physleta.2008.11.060
8. H. Zhang, J. Zhang, T. Xu, M. He and J. Li, *RSC Adv.*, **3**, 3535 (2013); https://doi.org/10.1039/c3ra22876b
9. X. Fang, T. Zhai, U.K. Gautam, L. Li, L. Wu, Y. Bando and D. Golberg, *Progr. Mater. Sci.*, **56**, 175 (2011); https://doi.org/10.1016/j.pmatsci.2010.10.001
10. A.A.A. Al-Zahra and A.K.M.A. Al-Sammarraie, *Chem. Methodol.*, **6**, 67 (2022); https://doi.org/10.22034/chemm.2022.1.7
11. G.H. Yue, P.X. Yan, D. Yan, X.Y. Fan, M.X. Wang, D.M. Qu and J.Z. Liu, *Appl. Phys., A Mater. Sci. Process.*, **84**, 409 (2006); https://doi.org/10.1007/s00339-006-3643-8
12. S. Biswas, S. Kar and S. Chaudhuri, *Synth. React. Inorg. Met.-Org. Nano-Met. Chem.*, **36**, 33 (2006); https://doi.org/10.1080/15533170500471417
13. P. Iranmanesh, S. Saeednia and M. Nourzpoor, *Chin. Phys. B*, **24**, 046104 (2015); https://doi.org/10.1088/1674-1056/24/4/046104
14. H. Moon, C. Nam, C. Kim and B. Kim, *Mater. Res. Bull.*, **41**, 2013 (2006); https://doi.org/10.1016/j.materresbull.2006.04.007
15. T. Xaba, M.J. Moloto and N. Moloto, *Mater. Lett.*, **146**, 91 (2015); https://doi.org/10.1016/j.matlet.2015.01.153
16. T.T.Q. Hoa, L.V. Vu, T.D. Canh and N.N. Long, *J. Phys. Conf. Ser.*, **187**, 012081 (2009); https://doi.org/10.1088/1742-6596/187/1/012081
17. N.H. Abdullah, Z. Zainal, S. Silong, M.I.M. Tahir, K.-B. Tan and S.-K. Chang, *Mater. Chem. Phys.*, **173**, 33 (2016); https://doi.org/10.1016/j.matchemphys.2016.01.034
18. Y. Ni, G. Yin, J. Hong and Z. Xu, *Mater. Res. Bull.*, **39**, 1967 (2004); https://doi.org/10.1016/j.materresbull.2004.01.011
19. N. Soltani, E. Saion, M. Erfani, K. Rezaee, G. Bahmanrokh, G.P.C. Drummen, A. Bahrami and M.Z. Hussein, *Int. J. Mol. Sci.*, **13**, 12412 (2012); https://doi.org/10.3390/ijms131012412
20. L.S. Archana and D.N. Rajendran, *Mater. Today Proc.*, **41**, 461 (2021); https://doi.org/10.1016/j.matpr.2020.05.227
21. A.A. Ebnalwaled, M.H. Essai, B.M. Hasaneen and H.E. Mansour, *J. Mater. Sci. Mater. Electron.*, **28**, 1958 (2017); https://doi.org/10.1007/s10854-016-5749-x
22. T. Xaba, M.J. Moloto, M. Al-Shakban, M.A. Malik, P. O'Brien and N. Moloto, *Mater. Sci. Semicond. Process.*, **71**, 109 (2017); https://doi.org/10.1016/j.mssp.2017.07.015
23. C. Díaz-Cruz, G. Alonso Nuñez, H. Espinoza-Gómez and L.Z. Flores-López, *Eur. Polym. J.*, **83**, 265 (2016); https://doi.org/10.1016/j.eurpolymj.2016.08.025
24. R. Finsy, *Langmuir*, **20**, 2975 (2004); https://doi.org/10.1021/la035966d